Thermalization, evolution and observables in integrated hydrokinetic model of A+A collisions

Yu. Sinyukov, BITP, Kiev

In collaboration with:
V. Naboka and Iu. Karpenko

NICA DAYS in WARSAW 2015
&
XI Workshop on Particle Correlations and Femtoscopy (WPCF 2015)
Warsaw, Poland, 03 - 07 November 2015

Integrated HydroKinetic model: HKM → iHKM

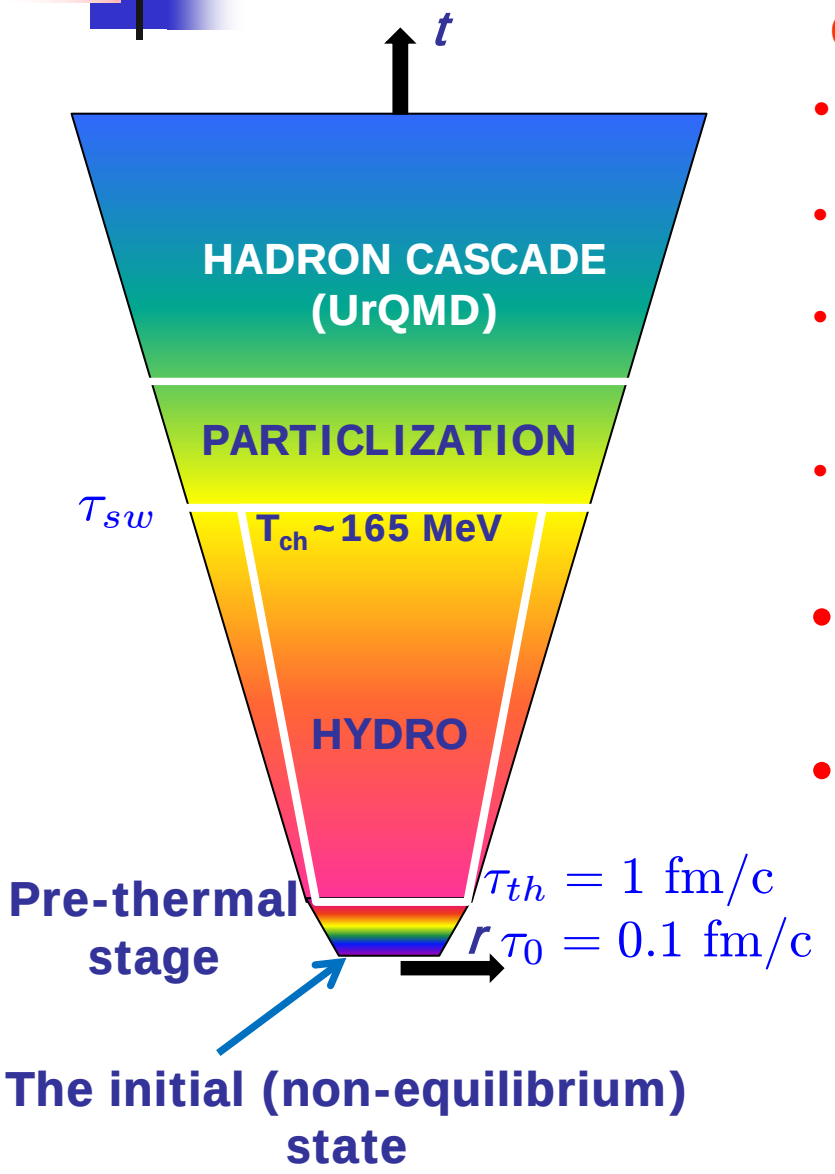

Complete algorithm incorporates the stages:

- **generation of the initial states**;
- **thermalization of initially non-thermal matter**;
- **viscous chemically equilibrium hydrodynamic expansion**;
- **sudden (with option: continuous) particlization of expanding medium**;
- **a switch to UrQMD cascade with near equilibrium hadron gas as input;**
- **simulation of observables.**

Yu.S., Akkelin, Hama: PRL 89 (2002) 052301;
... + Karpenko: PRC 78 (2008) 034906;
Karpenko, Yu.S. : PRC 81 (2010) 054903;
... PLB 688 (2010) 50;
Akkelin, Yu.S. : PRC 81 (2010) 064901;
Karpenko, Yu.S., Werner: PRC 87 (2013) 024914;
Naboka, Akkelin, Karpenko, Yu.S. : PRC **91** (2015) 014906;
Naboka, Karpenko, Yu.S. arXiv: 1508.07204 (subm. to PRC).

.

Initial states

The most commonly used models of initial state are:

High Energies

MC-G (Monte Carlo Glauber)
MC-KLN (Monte Carlo Kharzeev-Levin-Nardi)
EPOS (parton-based Gribov-Regge model)
EKRT (perturbative QCD + saturation model)
IP-Glasma (Impact Parameter dependent Glasma)

Low Energies

MC-G (Monte Carlo Glauber) - ?
UrQMD (Ultra-Relativistic Molecular Dynamics) - ?

PROBLEM:

No one model leads to the proper matter thermalization, while the biggest experimental discovery for a few decades is that hydrodynamics is the basis of the "Standard Model " of high energy A+A collisions

MC-G Initial State (IS) attributed to $\tau_0 = 0.1$ fm/c

GLISSANDO 2

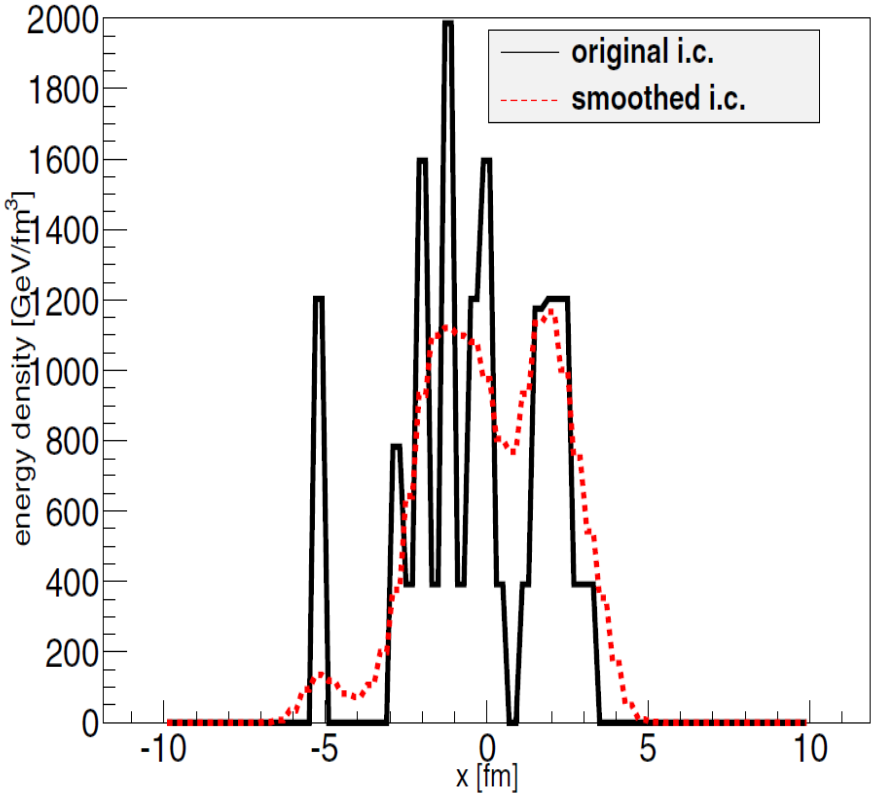

- The initial state (IS) is highly inhomogenious.
- It is not locally equilibrated.
- The IS most probable is strongly momentum anisotropic (result from CGC)

$$f(t_{\sigma_0}, \mathbf{r}_{\sigma_0}, \mathbf{p}) = \epsilon(b; \tau_0, \mathbf{r}_T) f_0(p)$$

$$T^{\mu\nu}_{\text{free}}(x) = \int d^3p \frac{p^\mu p^\nu}{p_0} f_{\sigma_0}(x,p); T^{00}[f_0(p)] = 1$$

$$f_0^*(p) \propto \exp\left(-\sqrt{\frac{p_T^2}{\lambda_\perp^2} + \frac{p_L^2}{\lambda_\parallel^2}}\right)$$

Florkowski et al

MC-G Hybrid for ensemble of ISs

$$\epsilon(b; \tau_0, \mathbf{r}_T) = \epsilon_0 \frac{(1-\alpha) N_W(b, \mathbf{r}_T)/2 + \alpha N_{bin}(b, \mathbf{r}_T)}{(1-\alpha) N_W(b=0, \mathbf{r}_T=0)/2 + \alpha N_{bin}(b=0, \mathbf{r}_T=0)}$$

Parameters of IS

$$\Lambda = \lambda_\perp / \lambda_\parallel$$

ϵ_0, α = 0.24 [4]

Multiplicity dependence of all charged particles on centrality

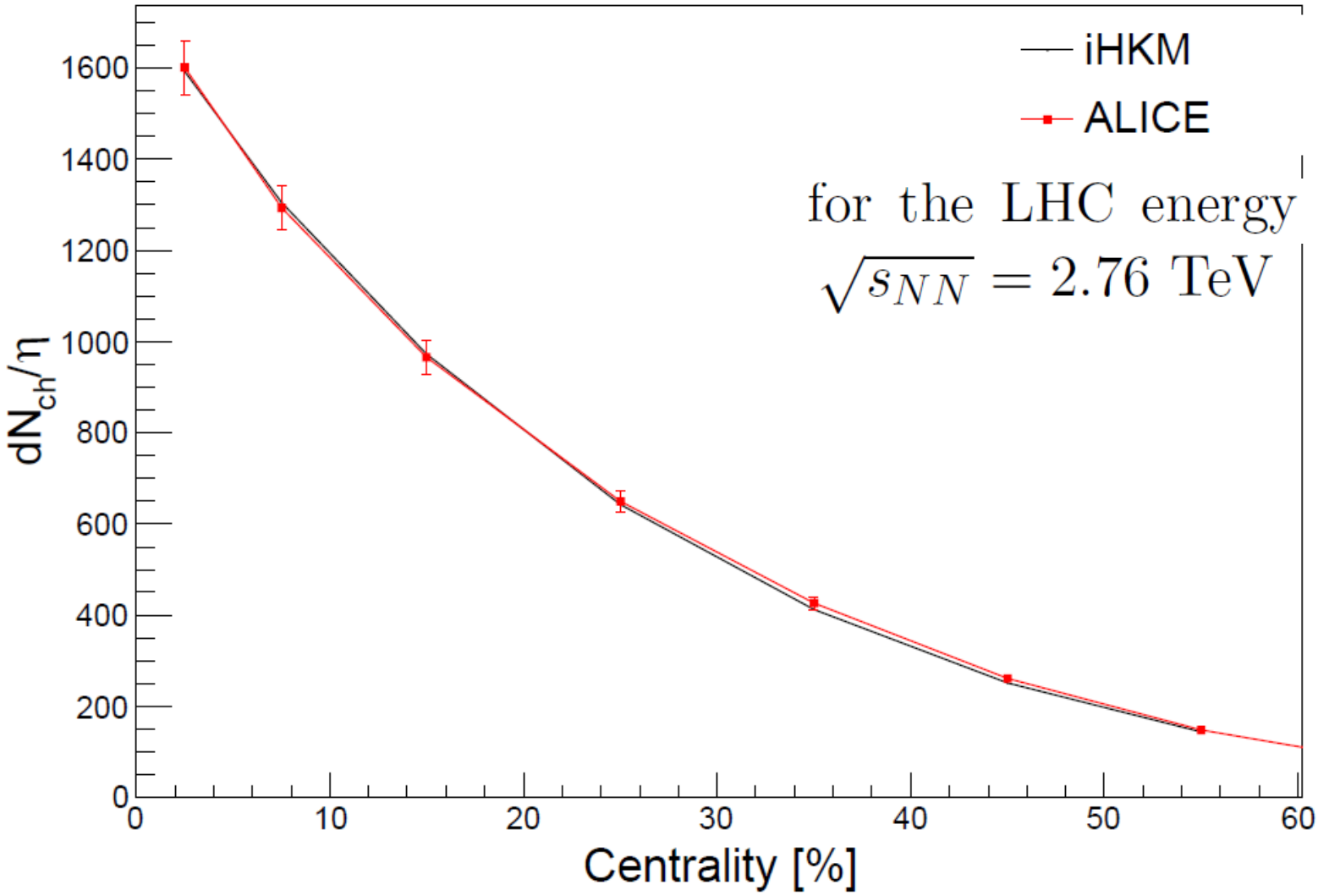

parameter values : $\tau_0 = 0.1$ fm/c, $\tau_{rel} = 0.25$ fm/c, $\eta/s = 0.08$, $\Lambda = 100$

Pre-thermal stage (thermalization)

Akkelin, Yu.S. :PRC **81** (2010); Naboka, Akkelin, Karpenko, Yu.S. : PRC **91** (2015).

Non-thermal state $\tau_0 = 0.1$ fm/c $\longrightarrow$ locally near equilibrated state $\tau_{th} = 1$ fm/c

Boltzmann equation in relaxation time approximation (integral form) **MAIN OBJECT**

$$\mathcal{P}_\sigma(x,p) = \exp\Big(-\int_t^{t_\sigma} \frac{d\bar{t}}{\tau_{rel}(\overline{x},p)}\Big)$$

$$\overline{x} \equiv (\bar{t}, \mathbf{x}_\sigma + (\mathbf{p}/p_0)(\bar{t} - t_\sigma))$$

MAIN ANSATZ with minimal number of parameters: $\tau_0,\ \tau_{th},\ \tau_{rel}$

$$\mathcal{P}_{\tau_0\to\tau}(\tau) = \left(\frac{\tau_{th}-\tau}{t_{th}-\tau_0}\right)^{\frac{\tau_{th}-\tau_0}{\tau_{\rm rel}(\tau_0)}} \Longrightarrow T^{\mu\nu}(x) = T^{\mu\nu}_{\rm free}(x)\mathcal{P}(\tau) + T^{\mu\nu}_{\rm hyd}(x)(1-\mathcal{P}(\tau))$$

$$\Longrightarrow 0 \le \mathcal{P}(\tau) \le 1,\ \mathcal{P}(\tau_0) = 1,\ \mathcal{P}(\tau_{th}) = 0,\ \partial_\mu \mathcal{P}(\tau)_{\tau_{\rm th}} = 0$$

MAIN EQUATIONS

$$\partial_{;\mu}\widetilde{T}^{\mu\nu}_{\rm hyd}(x) = -T^{\mu\nu}_{\rm free}(x)\partial_{;\mu}\mathcal{P}(\tau)$$

where $\begin{cases} \tilde{T}^{\mu\nu}_{\rm hyd} = [1-\mathcal{P}(\tau)]T^{\mu\nu}_{\rm hyd} \\ \widetilde{\pi}^{\mu\nu} = \pi^{\mu\nu}(1-\mathcal{P}) \end{cases}$

$$(1-\mathcal{P}(\tau))\left\langle u^\gamma \partial_{;\gamma}\frac{\widetilde{\pi}^{\mu\nu}}{(1-\mathcal{P}(\tau))}\right\rangle = -\frac{\widetilde{\pi}^{\mu\nu} - (1-\mathcal{P}(\tau))\pi^{\mu\nu}_{\rm NS}}{\tau_\pi} - \frac{4}{3}\widetilde{\pi}^{\mu\nu}\partial_{;\gamma}u^\gamma$$

$\Lambda = 1$ $\tau_{rel} = 0.5$ fm/c $\Lambda = 100$

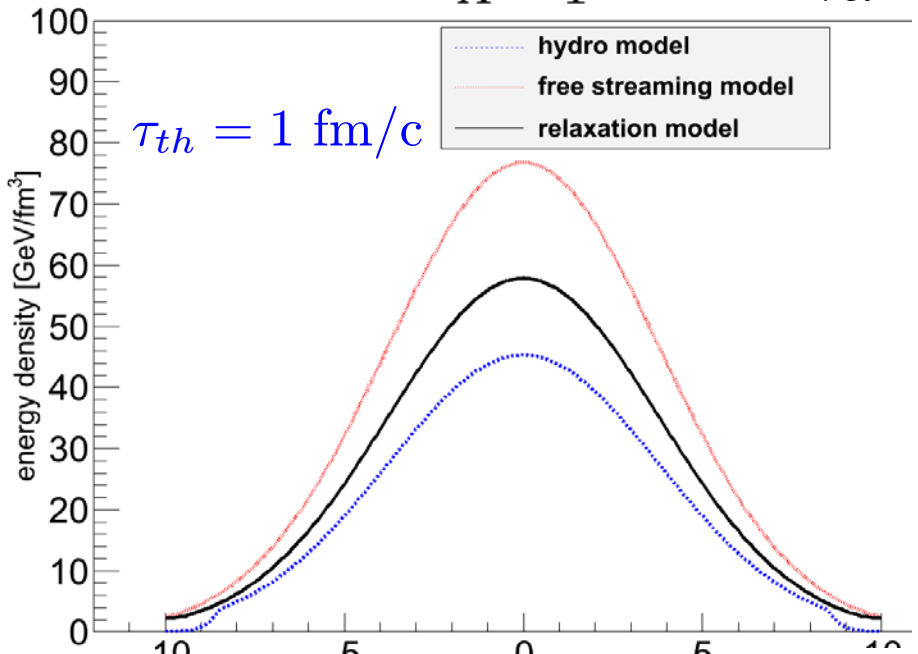

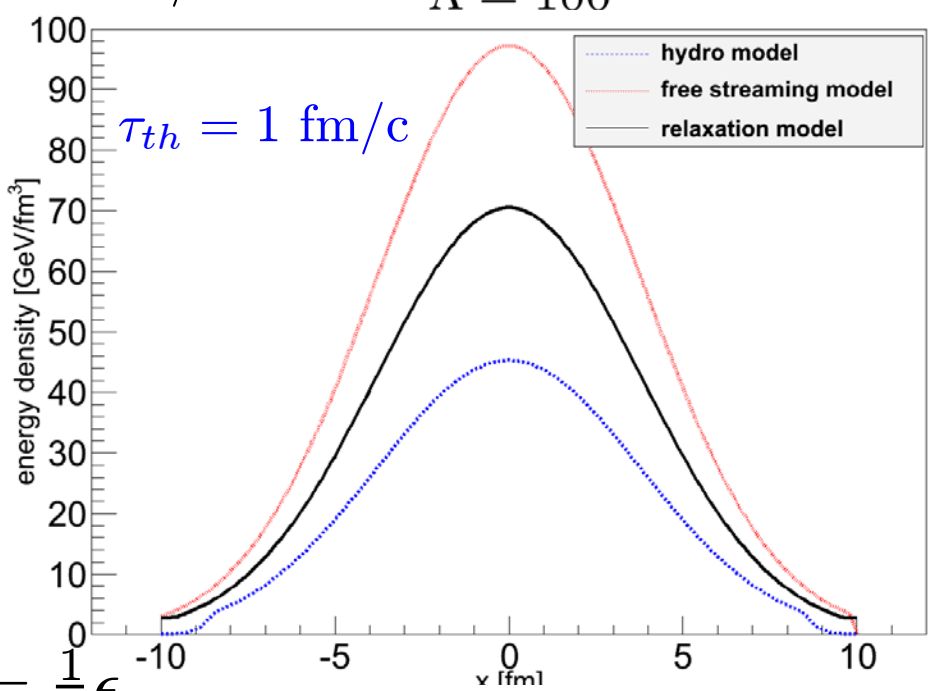

$p = \frac{1}{3}\epsilon$

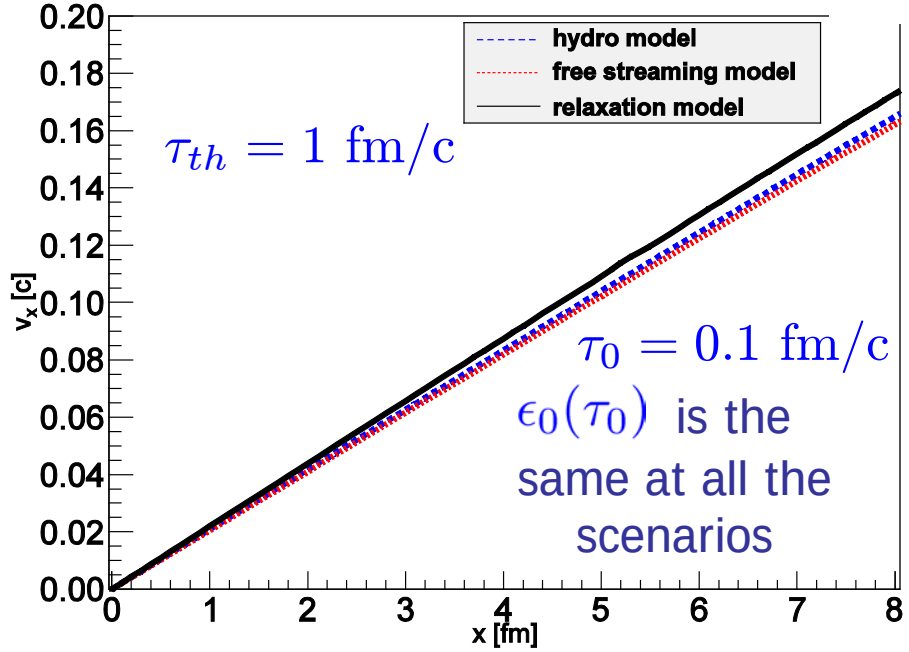

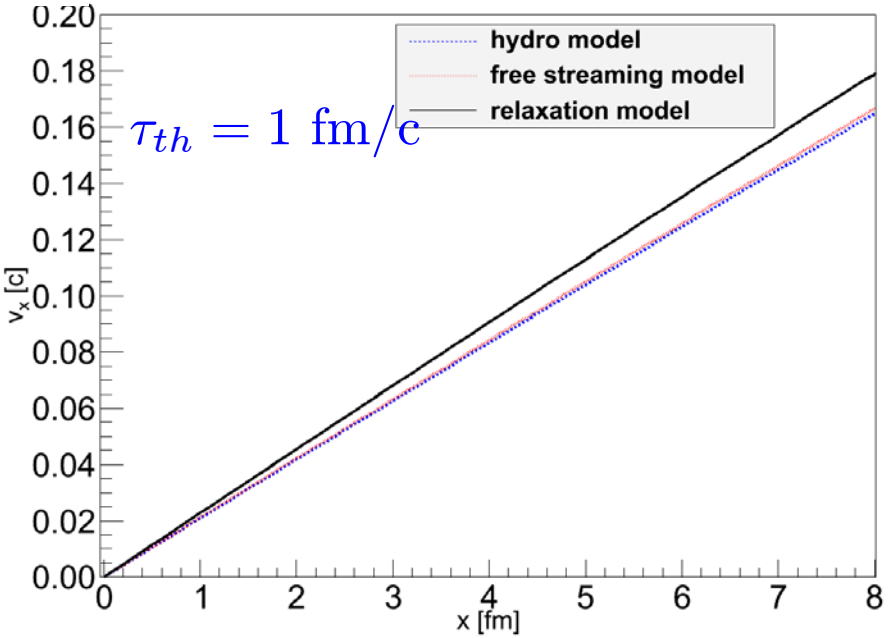

The other stages: Hydro evolution, particlization, hadronic cascade

- **Hydro evolution:** $\tau \leq \tau_{th}$ $T^{\mu\nu}(x) = T^{\mu\nu}_{\rm free}(x)\mathcal{P}(\tau) + T^{\mu\nu}_{\rm hyd}(x)(1-\mathcal{P}(\tau)) = T^{\mu\nu}_{\rm hyd}(x)$

$$= (\epsilon_{\rm hyd}(x) + p_{\rm hyd}(x) + \Pi)u^{\mu}_{\rm hyd}(x)u^{\nu}_{\rm hyd}(x) - (p_{\rm hyd}(x) + \Pi)g^{\mu\nu} + \pi^{\mu\nu}.$$

IC is the result of pre-thermal evolutuon reached at τ_{th}

Solving of Israel-Stewart Relativistic Viscous Fluid Dynamics with Π =0

The other stages: Hydro evolution, particlization, hadronic cascade

- **Hydro evolution:** $\tau \leq \tau_{th}$

$$T^{\mu\nu}(x) = T^{\mu\nu}_{\rm free}(x)\mathcal{P}(\tau) + T^{\mu\nu}_{\rm hyd}(x)(1-\mathcal{P}(\tau)) = T^{\mu\nu}_{\rm hyd}(x)$$
$$= (\epsilon_{\rm hyd}(x) + p_{\rm hyd}(x) + \Pi)u^{\mu}_{\rm hyd}(x)u^{\nu}_{\rm hyd}(x)$$
$$- (p_{\rm hyd}(x) + \Pi)g^{\mu\nu} + \pi^{\mu\nu}.$$

Solving of Israel-Stewart Relativistic Viscous Fluid Dynamics with Π =0

- **Particlization:** at the isotherm hypersurface T=165 MeV

$$\text{energy density } \epsilon = 0.5 \text{ GeV/fm}^3 \text{ for the Laine-Schroeder EoS}$$

Switching hypersurface build with help of Cornelius routine.

For particle distribution the Grad's 14 momentum ansatz is used:

$$\frac{d^3\Delta N_i}{dp^* d(cos\theta) d\phi} = \frac{\Delta\sigma^*_\mu p^{*\mu}}{p^{*0}} p^{*2} f_{eq}\left(p^{*0}; T, \mu_i\right)\left[1 + (1 \mp f_{eq})\frac{p^*_\mu p^*_\nu \pi^{*\mu\nu}}{2T^2(\epsilon + p)}\right]$$

The other stages: Hydro evolution, particlization, hadronic cascade

- **Hydro evolution:** $\tau \leq \tau_{th}$

$$T^{\mu\nu}(x) = T^{\mu\nu}_{\rm free}(x)\mathcal{P}(\tau) + T^{\mu\nu}_{\rm hyd}(x)(1-\mathcal{P}(\tau)) = T^{\mu\nu}_{\rm hyd}(x)$$
$$= (\epsilon_{\rm hyd}(x) + p_{\rm hyd}(x) + \Pi)u^{\mu}_{\rm hyd}(x)u^{\nu}_{\rm hyd}(x)$$
$$-(p_{\rm hyd}(x) + \Pi)g^{\mu\nu} + \pi^{\mu\nu}.$$

Solving of Israel-Stewart Relativistic Viscous Fluid Dynamics with Π =0

- **Particlization:** at the isotherm hypersurface T=165 MeV

$$\text{energy density } \epsilon = 0.5 \text{ GeV/fm}^3 \text{ for the Laine-Schroeder EoS}$$

Switching hypersurface build with help of Cornelius routine.

For particle distribution the Grad's 14 momentum ansatz is used:

$$\frac{d^3\Delta N_i}{dp^* d(cos\theta) d\phi} = \frac{\Delta\sigma^*_\mu p^{*\mu}}{p^{*0}} p^{*2} f_{eq}\left(p^{*0}; T, \mu_i\right)\left[1 + (1 \mp f_{eq})\frac{p^*_\mu p^*_\nu \pi^{*\mu\nu}}{2T^2(\epsilon + p)}\right]$$

- **Hadronic cascade:** The above distribution function with Poisson distributions for each sort of particle numbers is the input for UrQMD cascade.

The other stages: Hydro evolution, particlization, hadronic cascade

- **Hydro evolution:** $\tau \leq \tau_{th}$ $T^{\mu\nu}(x) = T^{\mu\nu}_{\rm free}(x)\mathcal{P}(\tau) + T^{\mu\nu}_{\rm hyd}(x)(1-\mathcal{P}(\tau)) = T^{\mu\nu}_{\rm hyd}(x)$

$$= (\epsilon_{\rm hyd}(x) + p_{\rm hyd}(x) + \Pi)u^{\mu}_{\rm hyd}(x)u^{\nu}_{\rm hyd}(x)$$

$$- (p_{\rm hyd}(x) + \Pi)g^{\mu\nu} + \pi^{\mu\nu}.$$

Solving of Israel-Stewart Relativistic Viscous Fluid Dynamics with Π =0

- **Particlization:** at the isotherm hypersurface T=165 MeV

energy density $\epsilon = 0.5$ GeV/fm^3 for the Laine-Schroeder EoS

Switching hypersurface build with help of Cornelius routine.

For particle distribution the Grad's 14 momentum ansatz is used:

$$\frac{d^3\Delta N_i}{dp^* d(cos\theta) d\phi} = \frac{\Delta\sigma^*_\mu p^{*\mu}}{p^{*0}} p^{*2} f_{eq}\left(p^{*0}; T, \mu_i\right)\left[1 + (1 \mp f_{eq})\frac{p^*_\mu p^*_\nu \pi^{*\mu\nu}}{2T^2(\epsilon + p)}\right]$$

- **Hadronic cascade:** The above distribution function with Poisson distributions for each sort of particle numbers is the input for UrQMD

Details are in: Naboka, Karpenko, Yu.S. arXiv: 1508.07204 (subm. to PRC).

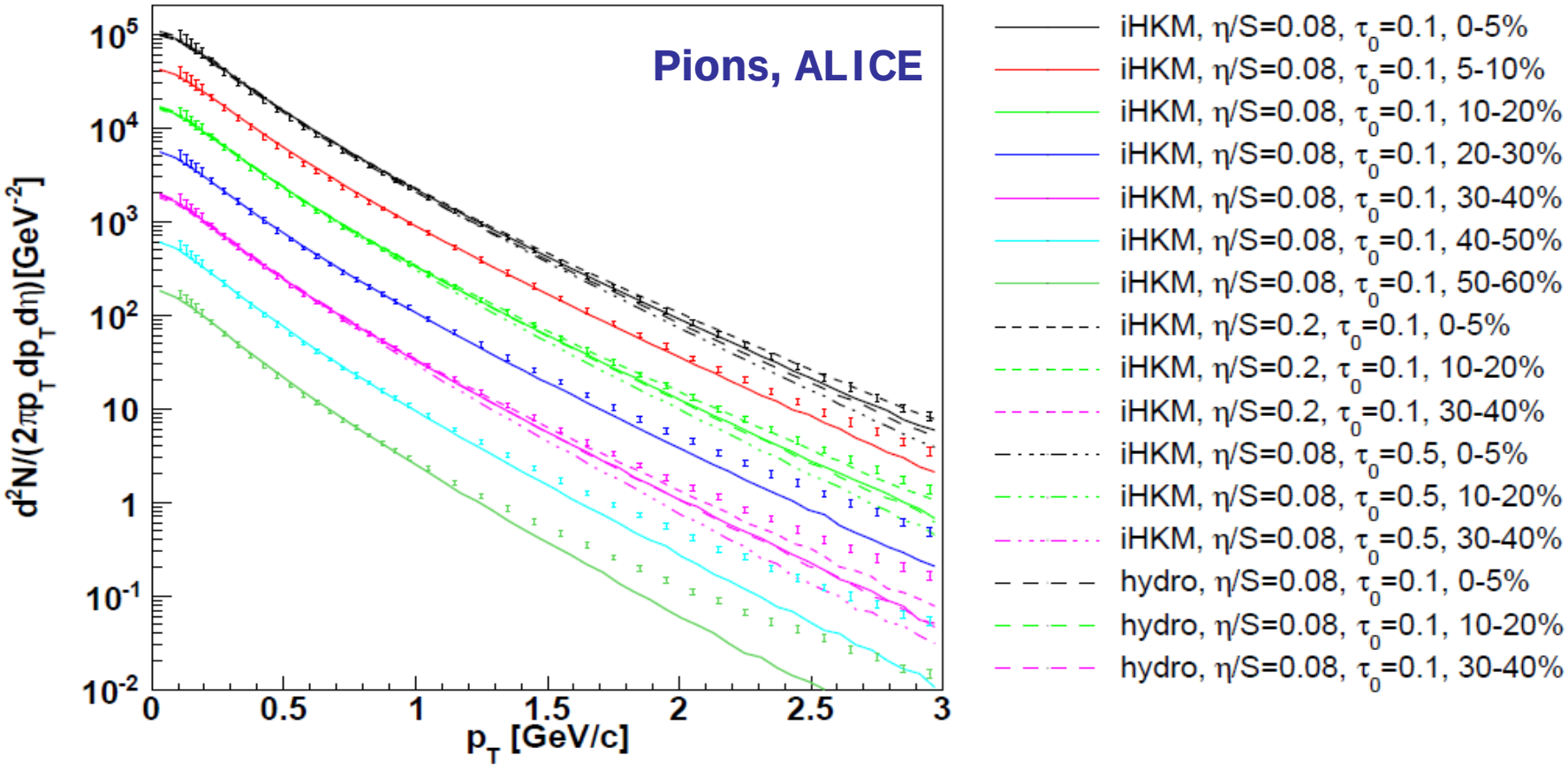

FIG. 2. Resulting pion spectra in the $0.1 < p_T < 3$ GeV/c region for centrality classes 0-5%, 5-10%, 10-20%, 20-30%, 30-40%, 40-50% and 50-60% obtained in the iHKM basic scenario (as in Fig. 1). The results are compared with those in iHKM at the other parameter $\tau_0 = 0.5$ fm/c and with pure viscous hydro at the starting time $\tau_{th} \to \tau_0 = 0.1$ fm/c for centrality classes 0-5%, 10-20%, 30-40%. The experimental data are from [31]. The spectra for different centralities are multiplied by the factor of 2 ($2^6 = 64$ for 0-5% centrality).

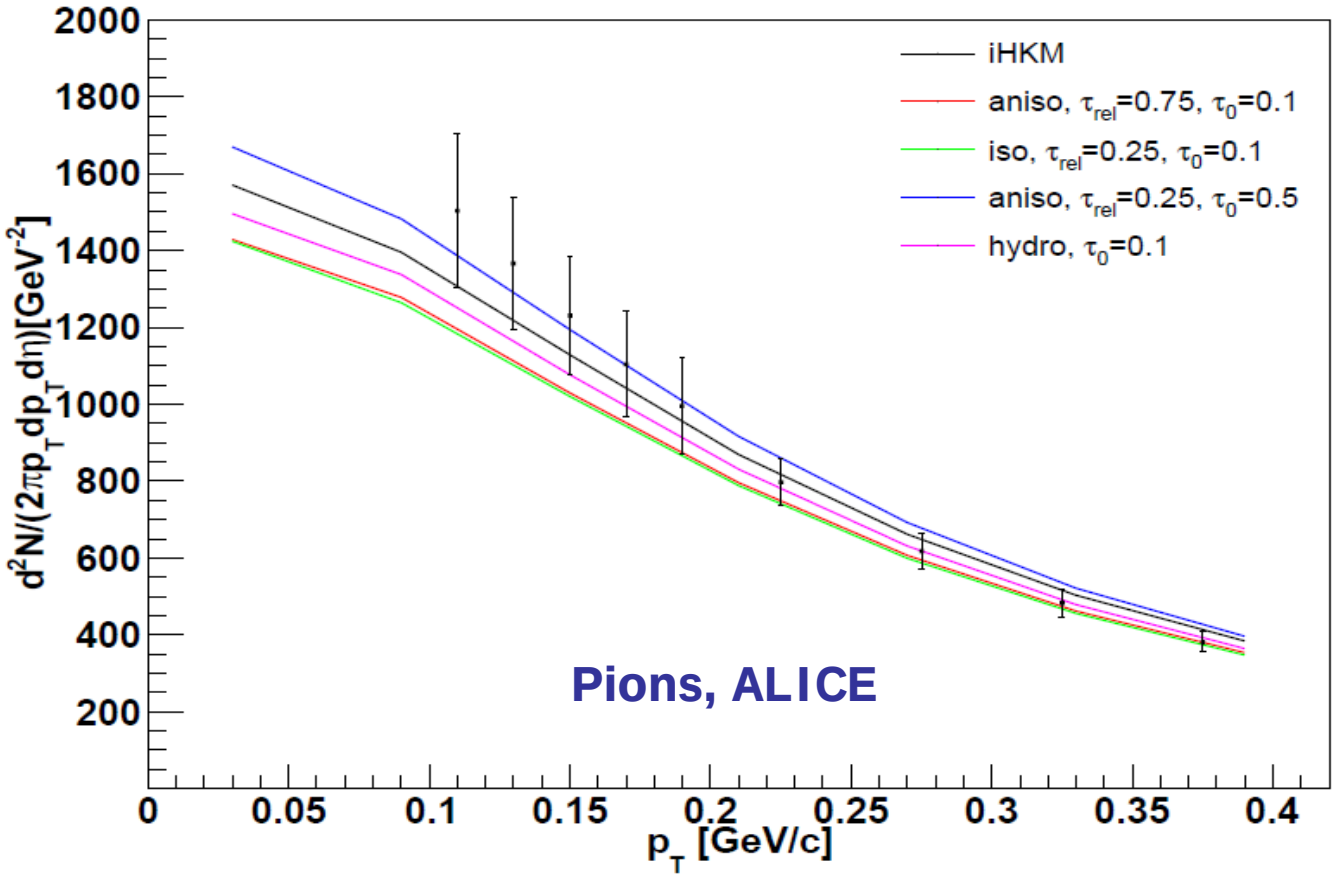

LHC,
Pion spectra
"under
microscope"
(linear scale)

FIG. 5. The detail picture of pion spectra in soft p_T region for 0-5% centrality in the iHKM basic scenario (as in Fig. 1) in comparison with the results obtained with (1) the other relaxation time $\tau_{rel} = 0.75$ fm/c instead of 0.25 fm/c, or with (2) isotropic parameter $\Lambda = 1$ instead of anisotropy one $\Lambda = 100$, or with (3) the other initial time $\tau_0 = 0.5$ fm/c instead of 0.1 fm/c. Also the results for pure viscous hydro, starting at $\tau_{th} \to \tau_0 = 0.1$ fm/c are presented. The experimental data are from [31].

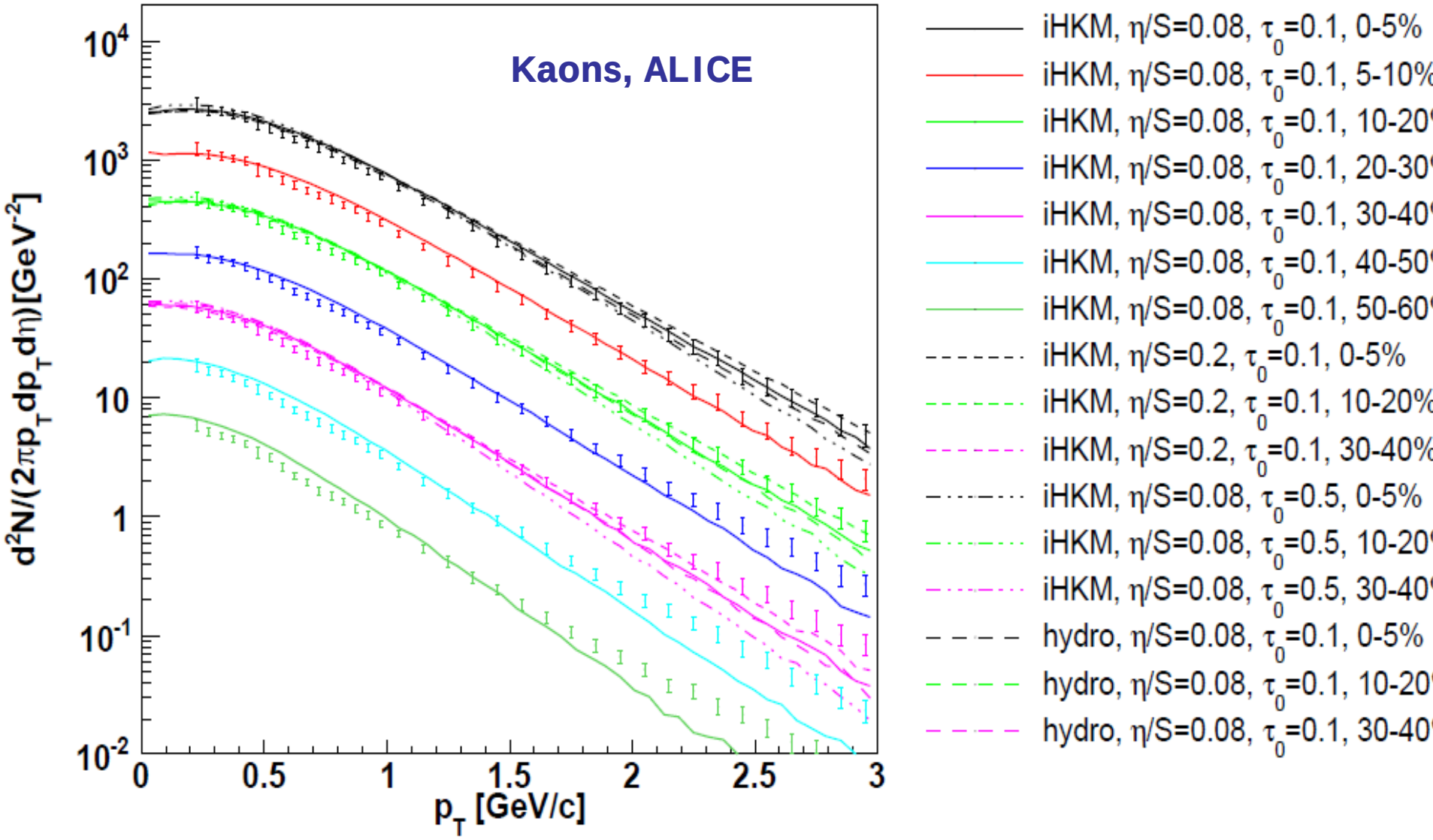

FIG. 3. The resulting kaon spectra under the same conditions as in Fig. 2.

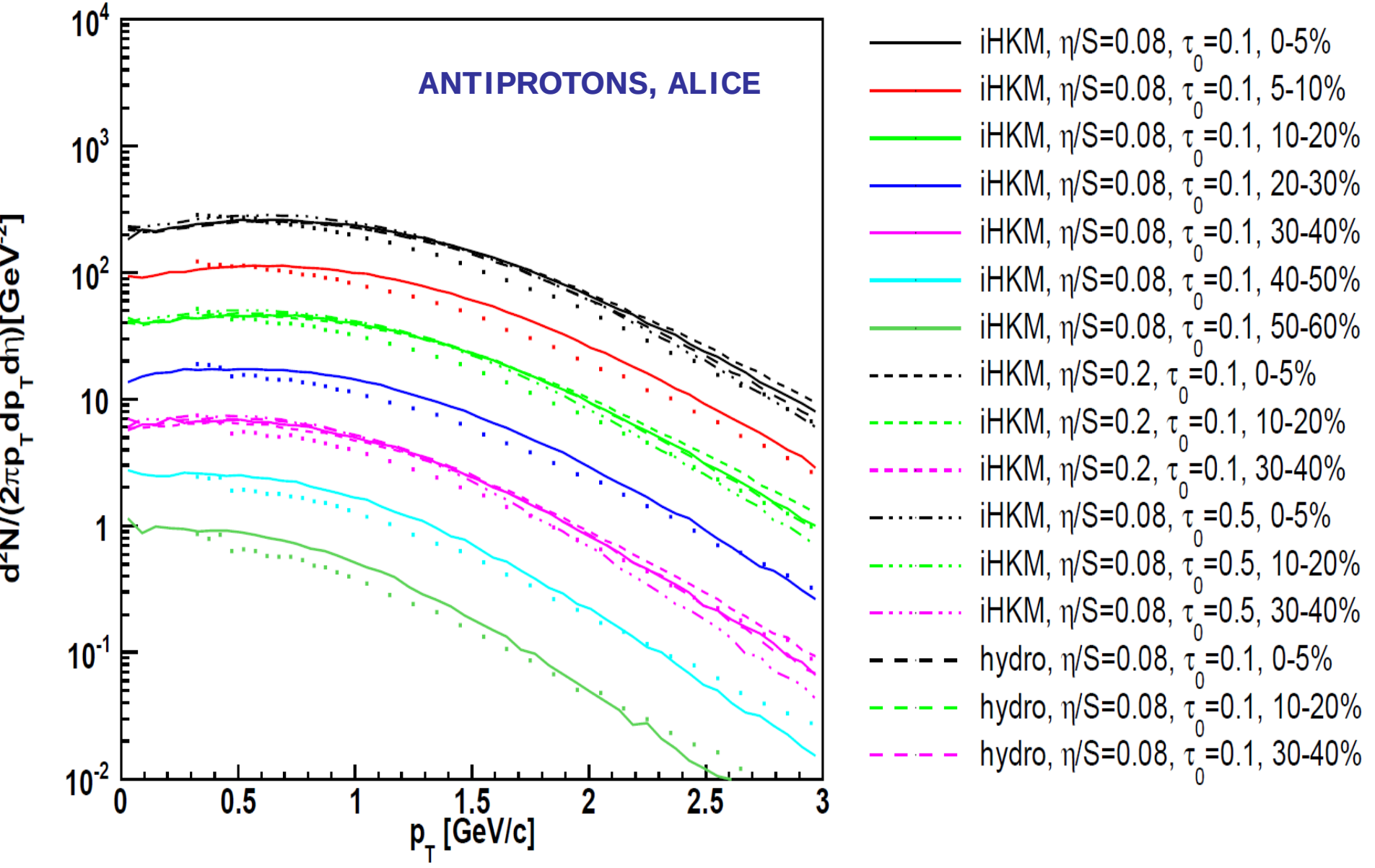

FIG. 4. The resulting antiproton spectra under the same conditions as in Fig. 2.

Predictions for particle spectra at LHC in non-central collisions

Centrality Dependence of π, K, p in Pb–Pb at $\sqrt{s_{NN}} = 2.76$ TeV

ALICE Collaboration

arXiv:1303.0737v1 [hep-ex]

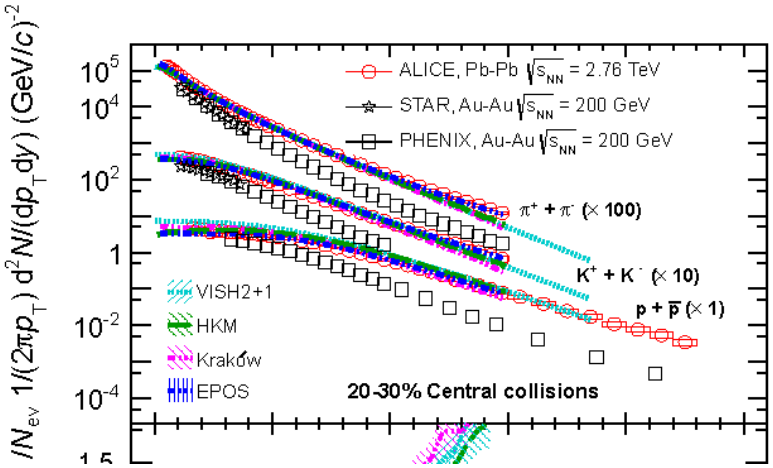

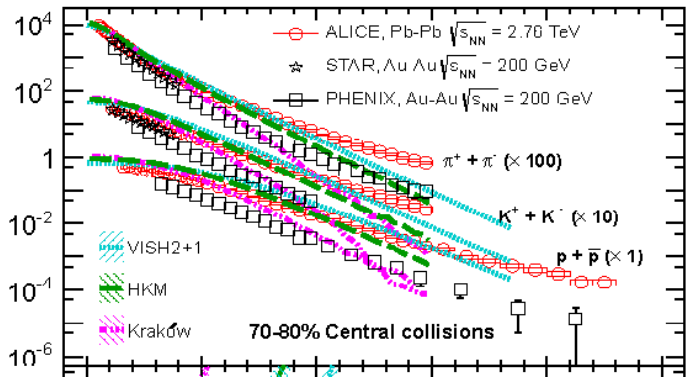

Quotations:

The difference between VISH2+1 and the data are possibly due to the lack of an explicit description of the hadronic phase in the model. This idea is supported by the comparison with HKM [47, 50]. HKM is a model similar to VISH2+1, in which after the hydrodynamic phase particles are injected into a hadronic cascade model (UrQMD), which further transports them until final decoupling. The hadronic phase builds up additional radial flow and affects particle ratios due to the hadronic interactions. As can be seen, this model yields a better description of the data. The protons at low p_T, and hence their total number, are rather well reproduced, even if the slope is significantly smaller than in the data. Antibaryon-baryon annihilation is an important ingredient for the description of particle yields in this model [47, 50].

.....

Phys. Rev. C 87, 024914 (2013)

[47] Y. Karpenko, Y. Sinyukov, and K. Werner, (2012), arXiv:1204.5351 [nucl-th]

[50] Y. Karpenko and Y. Sinyukov, J.Phys.G **G38**, 124059 (2011).

Predictions for particle yield at LHC in central collisions

Pion, Kaon, and Proton Production in Central Pb–Pb Collisions at $\sqrt{s_{NN}}$ = 2.76 TeV

The ALICE Collaboration* **Phys. Rev. Lett. 109, 252301 (2012)**

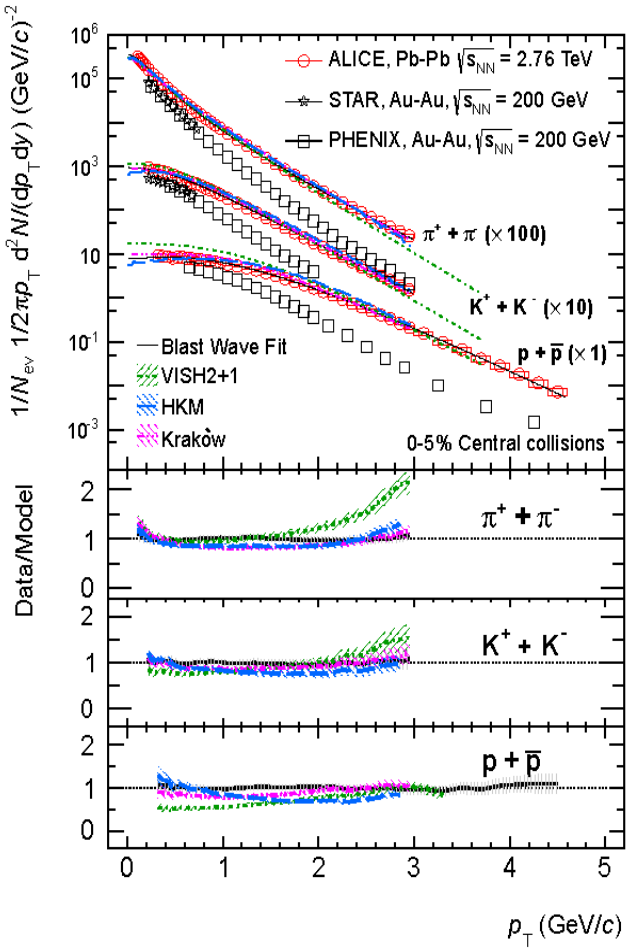

Quotations

This interpretation is supported by the comparison with HKM [39, 40], a similar model in which, after the hydrodynamic phase, particles are injected into a hadronic cascade model (UrQMD [41, 42]), which further transports them until final decoupling. The hadronic phase builds additional radial flow, mostly due to elastic interactions, and affects particle ratios due to inelastic interactions. HKM yields a better description of the data. At the LHC, hadronic final state interactions, and in particular antibaryon-baryon annihilation, may therefore be an important ingredient for the description of particle yields [43, 40], contradicting the scenario of negligible abundance-changing processes in the hadronic phase. The third model shown in Fig. 1 (Kraków [44, 45]) introduces non-equilibrium corrections due to viscosity at the transition from the hydrodynamic description to particles, which change the effective T_{ch}, leading to a good agreement with the data. In the region $p_T \lesssim 3$ GeV/c (Kraków) and $p_T \lesssim 1.5$ GeV/c (HKM) the last two models reproduce the experimental data within ~20%, supporting a hydrodynamic interpretation of the transverse momentum spectra at the LHC. These models also describe correctly other features of the space-time evolution of the system, as measured by ALICE with charged pion correlations [46].

[39] Y. Karpenko and Y. Sinyukov, J.Phys. **G38**, 124059 (2011), nucl-th/1107.3745.

[40] Y. Karpenko, Y. Sinyukov, and K. Werner, (2012), nucl-th/1204.5351.

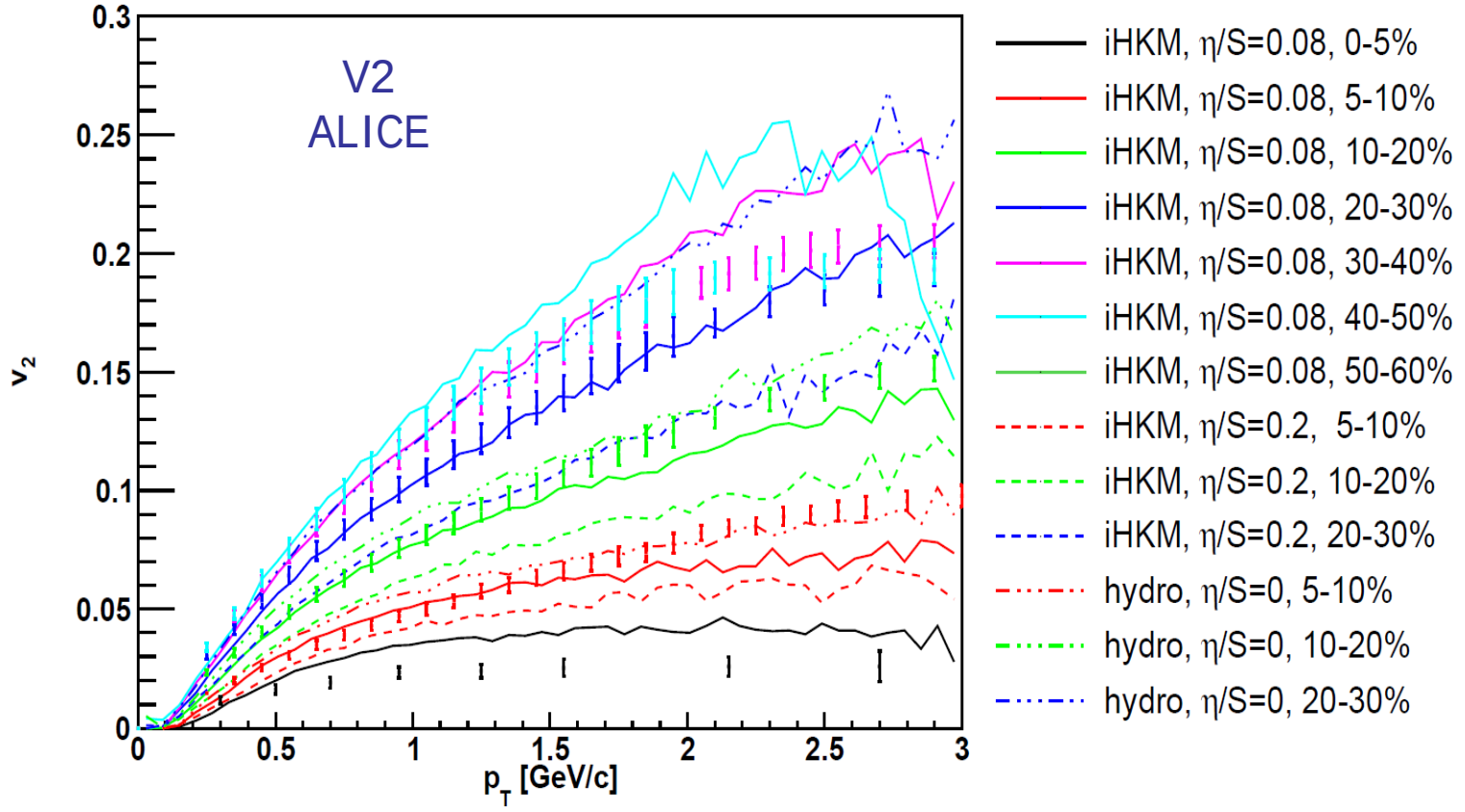

FIG. 6. All charged particles' v_2 coefficients centrality classes 0-5%, 5-10%, 10-20%, 20-30%, 30-40%, 40-50% and 50-60% obtained in the iHKM basic scenario (as in Fig. 1). The results are compared with those in iHKM at the other parameter dissipation condition, $\eta/s = 0.2$ instead of 0.08 and with ideal hydro with the starting time $\tau_{th} = \tau_0 = 0.1$ fm/c for centrality classes 5-10%, 10-20%, 20-30%. The experimental data are from [32].

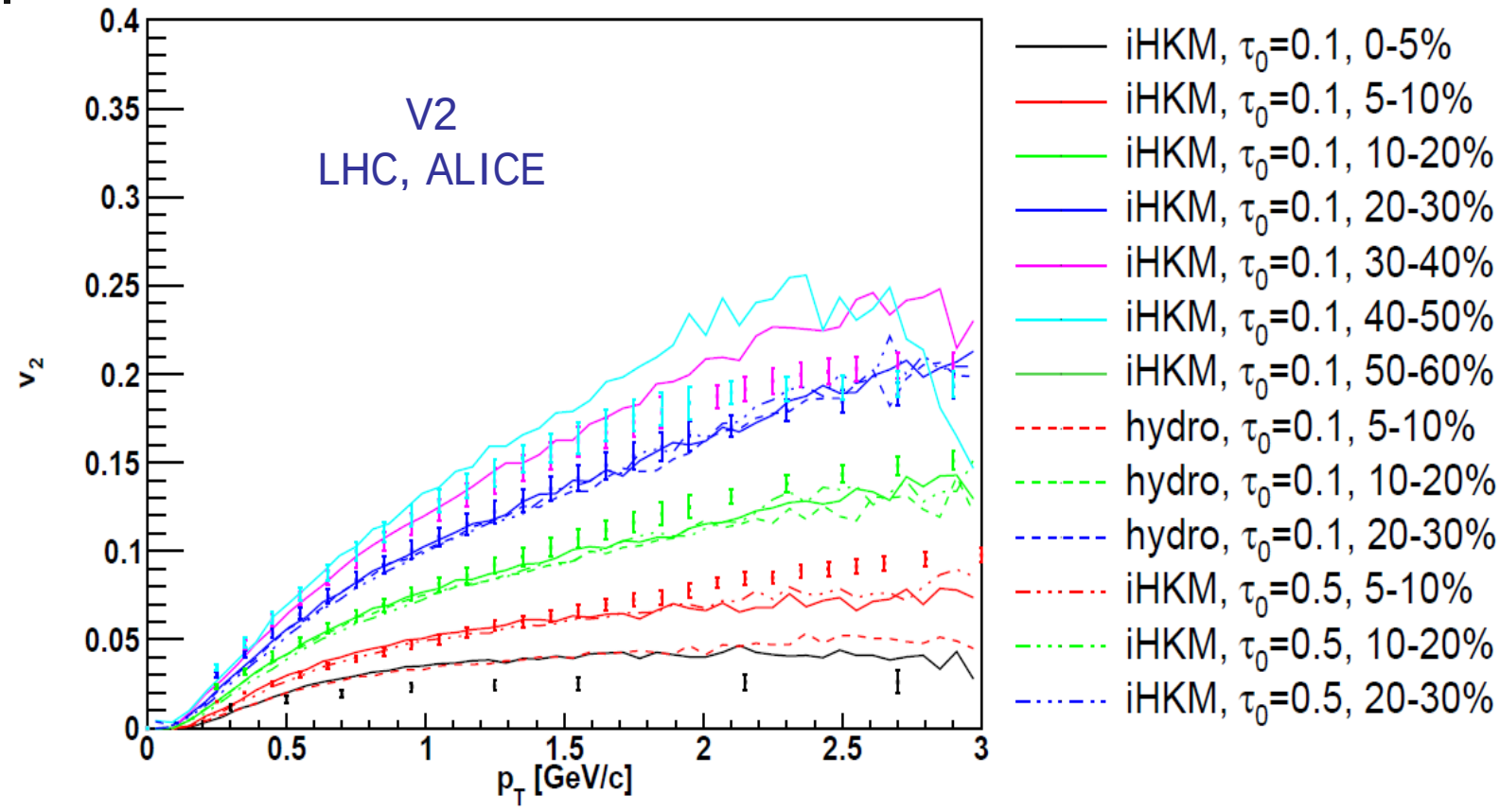

FIG. 7. All charged particles' v_2 coefficients centrality classes 0-5%, 5-10%, 10-20%, 20-30%, 30-40%, 40-50% and 50-60% obtained in the iHKM basic scenario (as in Fig. 1). The results are compared with those in iHKM at the other initial time, $\tau_0 = 0.5$ fm/c instead of 0.1 fm/c and with viscous hydro at the starting time $\tau_{th} = \tau_0 = 0.1$ fm/c for centrality classes 5-10%, 10-20%, 20-30%. The experimental data are from [32].

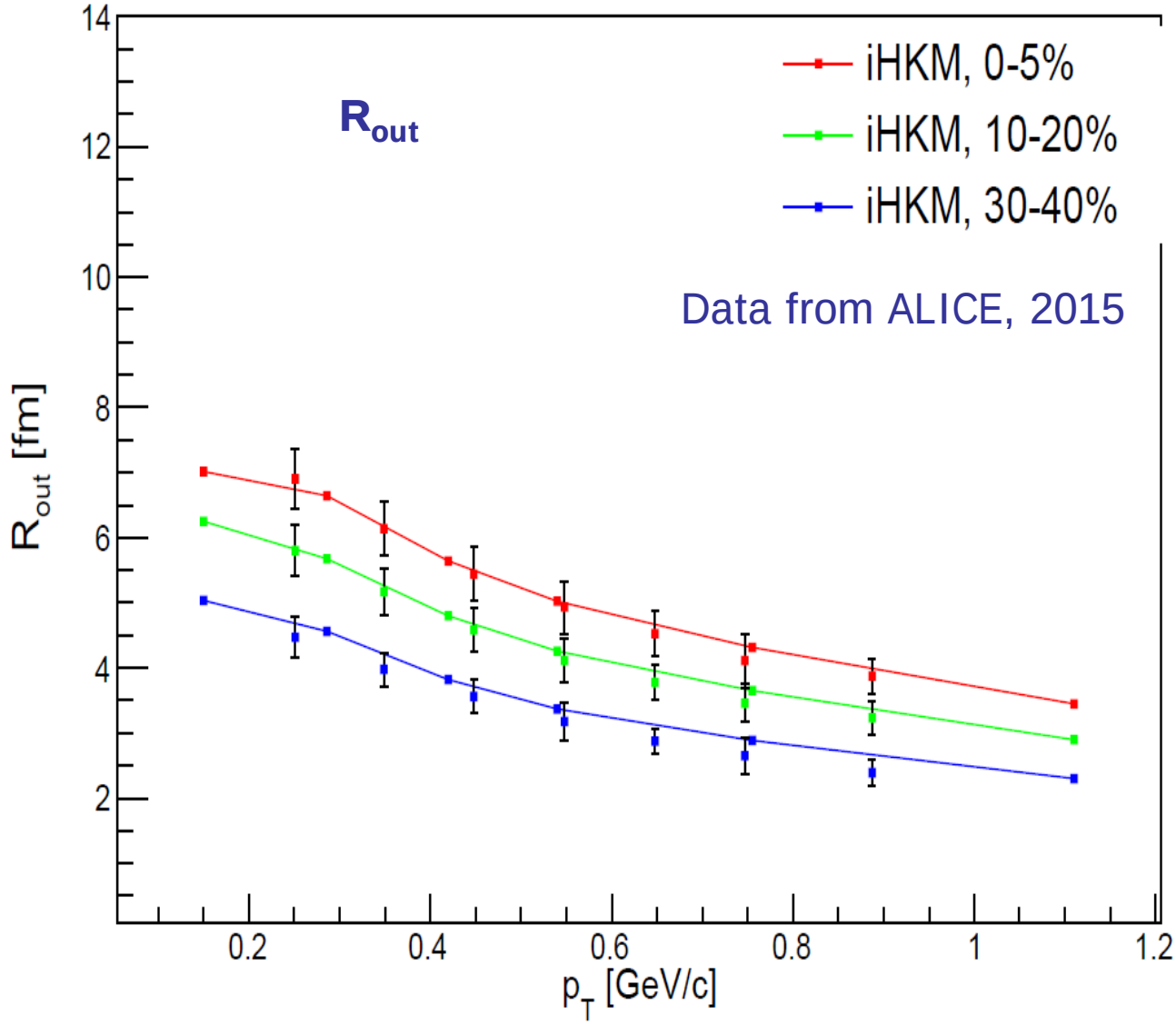

FIG. 8. The R_{out} dependence on transverse momentum for different centralities in the iHKM basic scenario under the same conditions as in Fig. 1.

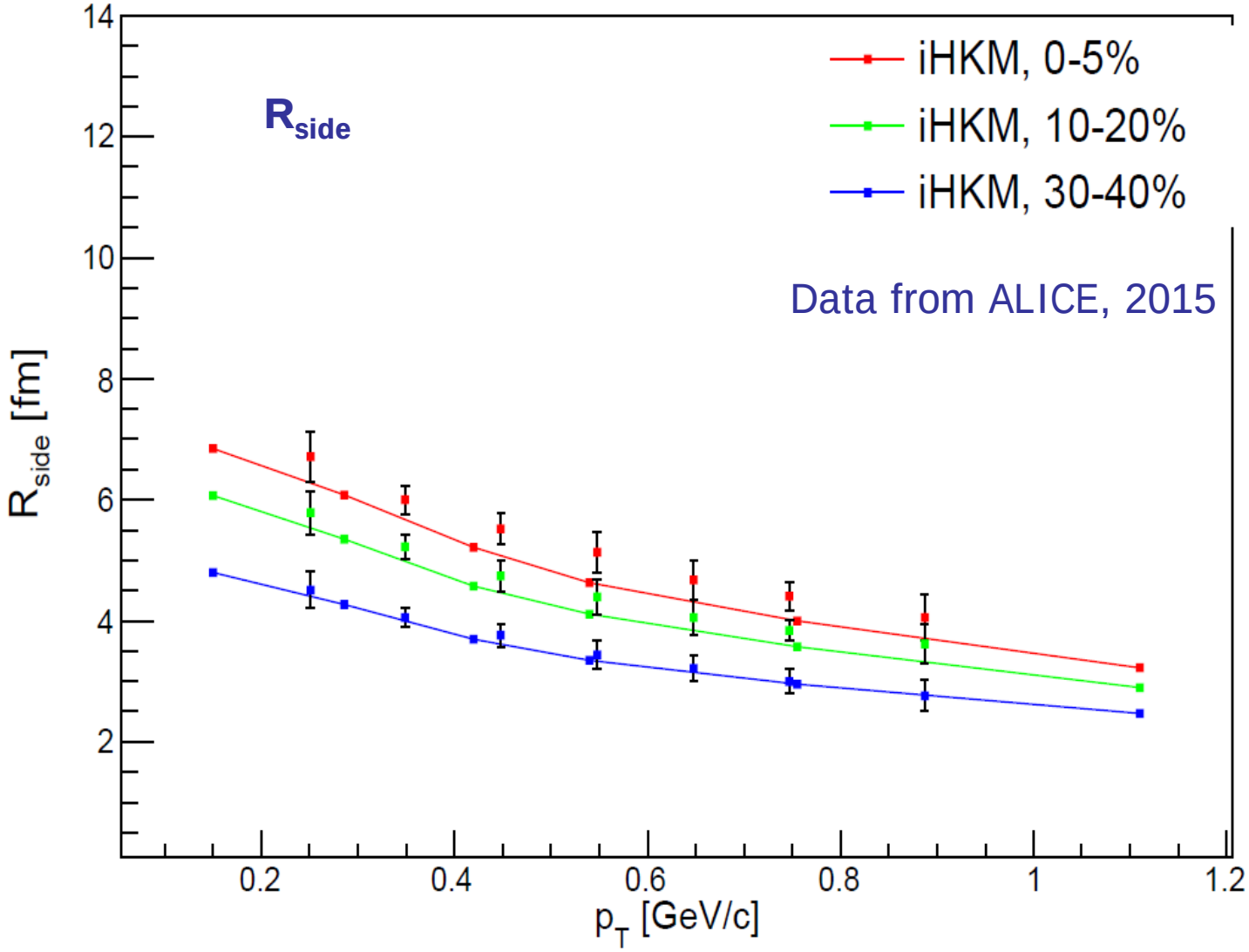

FIG. 9. The R_{side} dependence on transverse momentum for different centralities in the iHKM scenario under the same conditions as in Fig. 1. The experimental data are from [33].

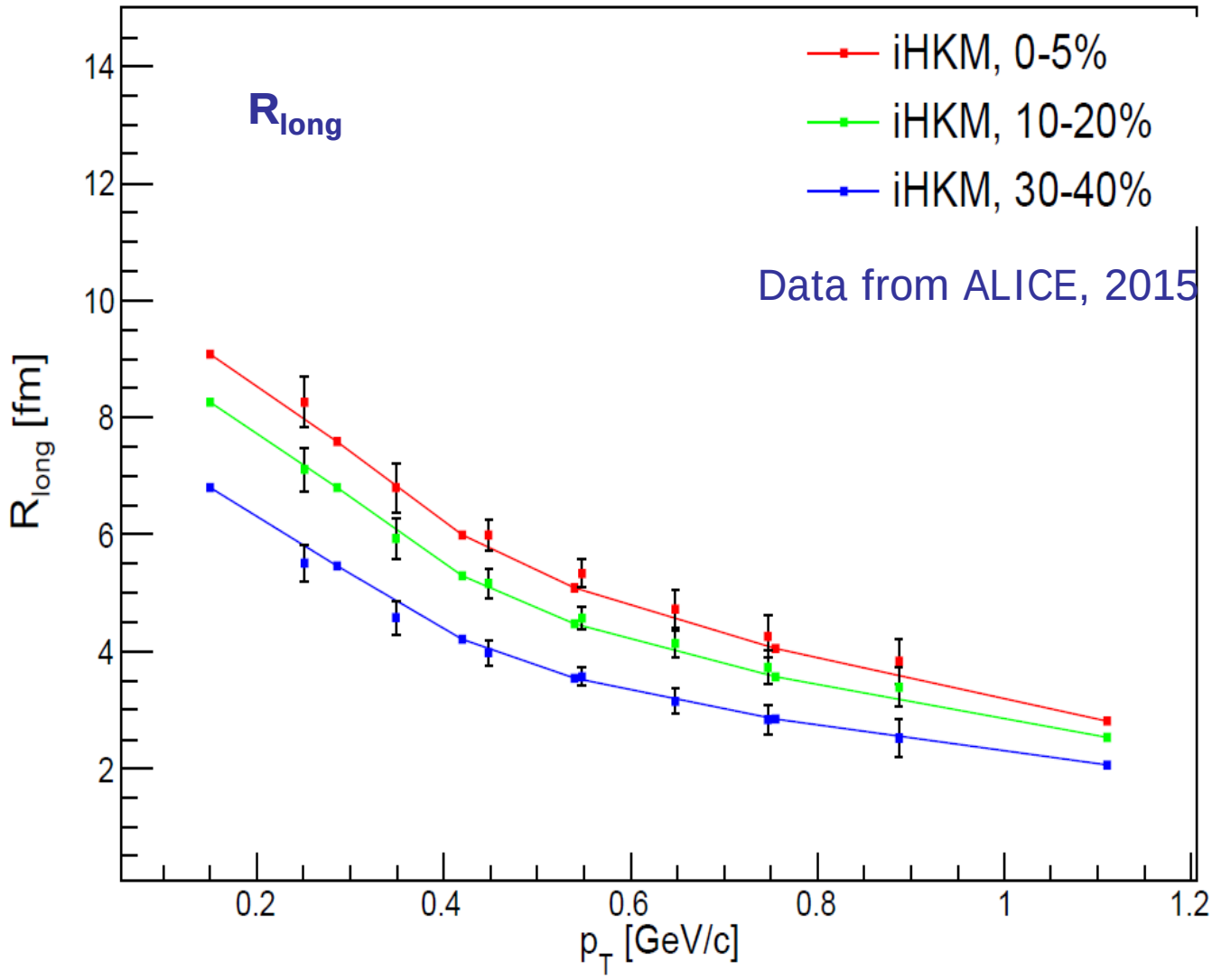

FIG. 10. The R_{long} dependence on transverse momentum for different centralities in the iHKM basic scenario - the same conditions as in Fig. 1. The experimental data are from [33].

Important results

The $\frac{dN_{ch}}{d\eta}(c)$ is OK at fixed relative contribution of binary collision $\alpha = 0.24$.

but at different max initial energy densities when other parameters change:

The two values of the shear viscosity to entropy is used for comparison:

$$\eta/s = 0.08 \approx \frac{1}{4\pi} \text{ and } \eta/s = 0.2$$

The basic result (selected by red) is compared with results at other parameters, including viscous and ideal pure thermodynamic scenarios (starting at τ_0 without pre-thermal stage but with subsequent hadronic cascade).

model	Λ	τ_{rel}	η/S	τ_0	ϵ_0 [GeV/fm^3]
hydro	-	-	0	0.1	1076.5
hydro	-	-	0.08	0.1	738.8
iHKM	1	0.25	0.08	0.1	799.5
iHKM	100	0.25	0.08	0.1	678.8
iHKM	100	0.75	0.08	0.1	616.5
iHKM	100	0.25	0.2	0.1	596.9
iHKM	100	0.25	0.08	0.5	126.7

The values τ_0, τ_{rel} corespond to fm/c.

No dramatic worsening of the results happens if simultaneously with changing of parameters/scenarios renormalize maximal initial energy density.

Summary

- The integrated hydrokinetic model (iHKM) of A+A collisions is developed.
- Quite satisfactory results at different centralities are reached for multiplicities of all charged particles, pion, kaon and antiproton spectra, pion *v*_2- coefficients and interferometry radii vs transverse momentum.
- The coherent description of these observables is achieved in iHKM with the small time formation (τ_0 = 0.1 fm/c) of the maximally anisotropic initial state, with small mean relaxation time, τ_{rel} = 0.25 fm/c, and the minimal ratio of shear viscosity over entropy density $\eta/s = 1/4\pi$.
- It is observed that the isotropic initial conditions, larger relaxation time, or treatment of the pre-thermal stage just with viscous or ideal hydro-approach, leads not to dramatically worse results, if normalization of maximal initial energy densities is adjusted to reproduce multiplicity of all charged particles in each scenario.
- It can explain a rather satisfactory data description in numerous variants of hybrid models without pre-thermal stage when the initial energy densities are defined up to a common factor.

Predictions for $\bar{p}\Lambda$ correlation function with purity corrected CF and residual correlations at the LHC

RHIC V. M. Shapoval, B. Erazmus,R. Lednicky, Yu.S. PRC **92**, 034910 (2015)

LHC V. M. Shapoval, Yu.S., V. Naboka PRC **92**, 044910 (2015)

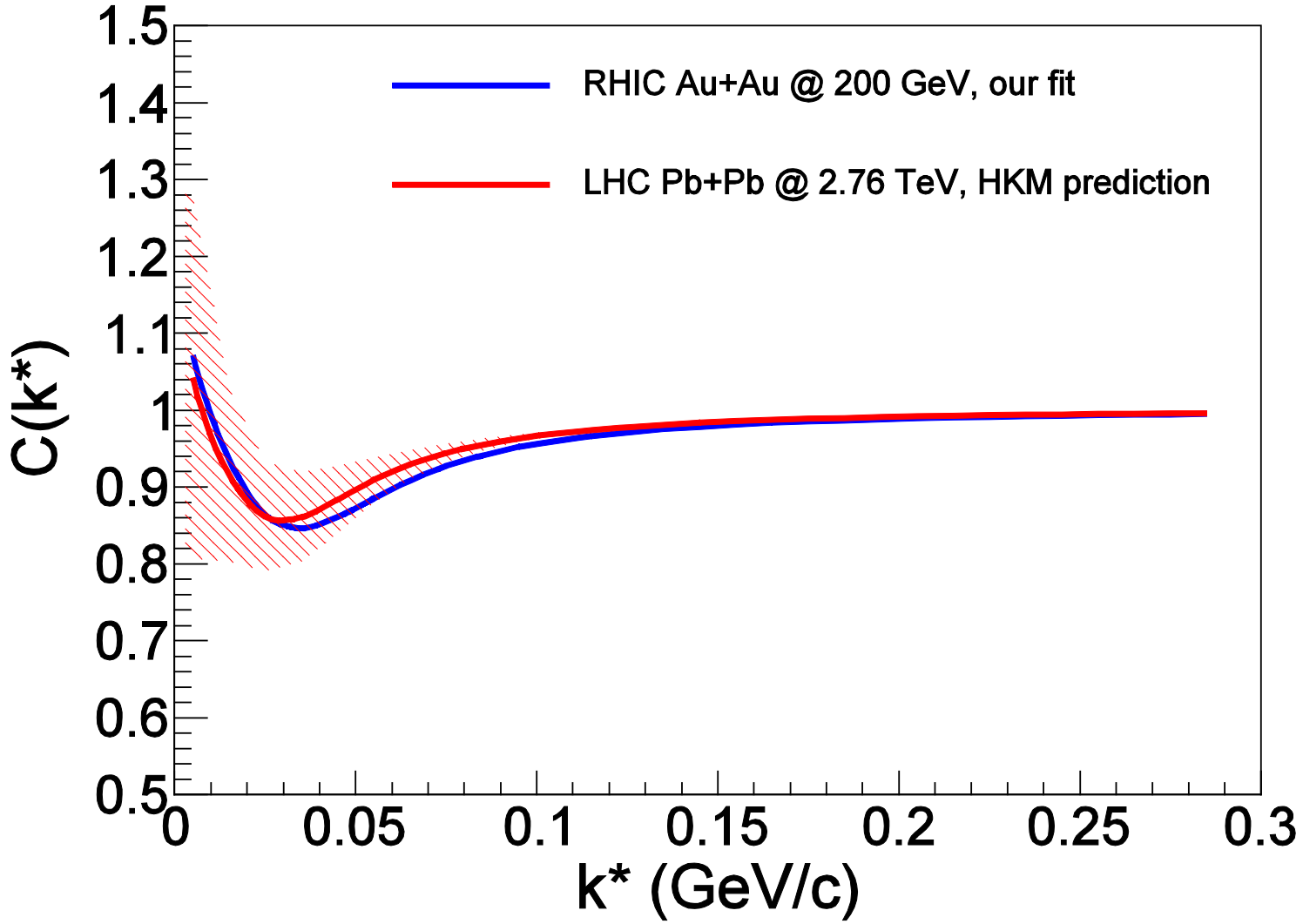

Thank you for your attention!